SEISMIC STABILITY ANALYSIS OF THREE DIMENSIONAL SLOPES USING ACCEPTABLE STRESS FIELDS[*]

A. TOTONCHI[1,**] F. ASKARI[2] AND O. FARZANEH[3]

[1]Dept. of Civil Engineering, Marvdasht Branch, Islamic Azad University, Marvdasht, I. R. of Iran
Email: Arash_Totonchi@yahoo.com
[2]Iran International Earthquake Engineering Institute, Tehran, I. R. of Iran
[3]Dept. of Civil Engineering, Tehran University, Tehran, I. R. of Iran

Abstract– Presented is a method of three-dimensional stability analysis of slopes due to earthquake forces based on the Lower-bound theorem of the limit analysis approach. The method's aim is to determine the factor of safety of such slopes using numerical linear finite element and lower bound limit analysis to produce seismic stability charts for three dimensional (3D) homogeneous slopes. The rigorous limit analysis results in this paper together with results of other researchers were found to bracket the slope stability number and therefore can be used to benchmark for solutions from other methods. It was found that using a two dimensional (2D) analysis to analyze a 3D problem will lead to a significant difference in the factors of safety depending on the slope geometries. Numerical 3D seismic results of the proposed algorithm are presented in the form of some dimensionless graphs which can be a convenient tool to be used by practicing engineers to estimate the initial stability for excavated or man-made slopes.

Keywords– Three-dimensional slope, slope stability, limit analysis, Lower-bound, limit equilibrium

1. INTRODUCTION

Limit-equilibrium analysis has been the most popular method for slope stability calculations. A major advantage of this approach is that complex soil profiles, seepage, and a variety of loading conditions can be easily dealt with. Two dimensional (2D) limit equilibrium analyses, such as Bishop's simplified method [1] and Janbu's simplified method [2], are two of the most popular approaches used to evaluate slope stability. It is commonly believed that 2D solutions utilized in design will obtain a conservative evaluation for a three dimensional (3D) slope failure. However, as pointed out by Gens et al. [3], estimates of the mobilized shear strength derived from the 2D back analysis for a 3D slope, will be unsafe.

In order to account for the three dimensional effects on slope stability many 3D methods have been proposed. The majority of methods proposed in these studies are simply based on extensions of Bishop's simplified [2], Spencer's [4], or Morgenstern and Price's [5] original 2D limit equilibrium slice methods. Many comparisons of limit-equilibrium methods indicate that techniques that satisfy all conditions of global equilibrium give similar results. Regardless of the different assumptions about the interslice forces, these methods give values of the safety factor that differ by no more than 5%. Even though it does not satisfy all conditions of global equilibrium, Bishop's simplified method also gives very similar results. Partly because of this and partly because of its simplicity, the slice method of limit-equilibrium analysis proposed by Bishop [2] has been used widely for predicting slope stability. Because of the approximate and somewhat arbitrary nature of limit-equilibrium analysis, concern is often voiced about how accurate these types of solutions really are. Using the limit theorems cannot only provide a simple and useful way

---

of analyzing the stability of geotechnical structures, but also avoids the shortcomings of the arbitrary assumptions underpinning the LEM. In most cases it is not feasible to perform a full displacement finite element analysis and as such the three dimensional effects of the slope in question are often ignored. However, ignoring the 3D effects when analyzing slopes can lead to unsafe answers. In the back analyses of shear strengths, for example, neglecting the 3D effects, will lead to values that are too high, and therefore affect any further stability assessments at the same location. As stated previously, one aim of this study is to produce 3D stability seismic and static charts that can be used by practicing engineers, extending those currently used regularly for 2D slope stability evaluation.

Currently, accepted three dimensional stability analysis solutions of slopes, available for practicing geotechnical engineers are few. This paper is devoted to use linear finite element, lower-bound solution method and an optimization approach to make the maximum lower bound solutions for 3D seismic slope stability.The main purpose of this paper is to provide sets of 3D seismic and static stability charts for homogeneous soil slopes by using the finite element bounding methods and upper-bound results of Farzaneh and Askari [6, 7] which can bracket the actual stability numbers from above and below.

2. BACKGROUND

Numerous methods have been proposed for three dimensional slope stability analysis. In general, these methods can be classified into the following types: (1) limit equilibrium approach (LEM) which is the most common; (2) numerical solutions based on the finite element method (FEM); and (3) limit analysis approach. Other methods of analysis, like the finite difference method, distinct element method, and probability assessment are also used in current slope stability analyses. Duncan [8] provides a comprehensive review for two dimensional (2D) and three dimensional (3D) LEM and FEM estimates of slope stability, and therefore the review of literature herein will be referring to more recent publications (post 1996).

- *Limit analysis*

The bound theorems of limit analysis are particularly useful if both upper and lower bound solutions can be calculated, because the true collapse load can then be bracketed from above and below. This feature is invaluable in cases for which an exact solution cannot be determined (such as slope stability problems), because it provides a built-in error check on the accuracy of the approximate collapse load.

Figure 1 shows a typical load-displacement curve as it might be measured for a surface footing test. The curve consists of an elastic portion; a region of transition from mainly elastic to mainly plastic behavior; a plastic region, in which the load increases very little while the deflection increases manifold; and finally, a work-hardening region. In a case of limit analysis, there exists no physical collapse load. However, to know the load at which the footing will deform excessively has obvious practical importance. For this purpose, idealizing the soil as a perfectly plastic medium and neglecting the changes in geometry lead to the condition in which displacements can increase without limit while the load is held constant as shown in Fig. 1.
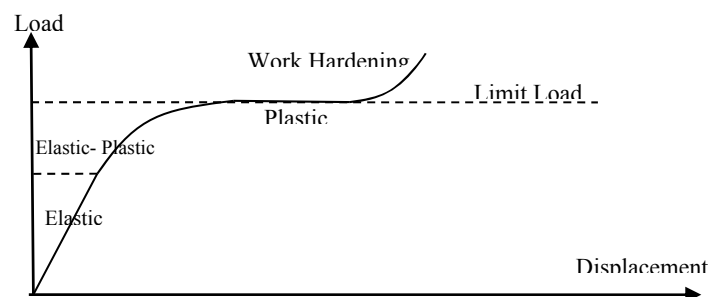

Fig. 1. Perfect plastic load-displacement diagram [17]

Although the limit theorems provide a simple and useful way of analyzing the stability of geotechnical structures, they have not been widely applied to the 3D slope stability problem. Currently, most slope stability evaluations based on the limit theorems have used the upper bound method alone, such as Chen et al. [9, 10], Donald and Chen [11], Farzaneh and Askari [6], De Buhan and Garnier [12], Michalowski [13,14], and Viratjandr and Michalowski [15]. Major contributions for soil slope stability analysis were presented by Michalowski and his co-worker who investigated local footing load effects on the 3D slope stability [5] and provided sets of stability charts for cohesive-frictional slopes which took seismic loadings and pore pressure into account. In addition, Michalowski [16] employed the limit analysis technique to estimate the stability of uniformly reinforced slopes. Because of the difficulties of constructing statically admissible stress fields manually, the application of limit analysis has in the past almost exclusively concentrated on the upper bound method. Although the upper bound solutions may be used as an estimate for the true collapse load, it is the lower bound solutions that are generally more useful in practice, because they are inherently conservative.

A lower bound solution is obtained by insisting that the stresses obey equilibrium and satisfy both the stress boundary conditions and the yield criterion. Each of these requirements imposes a separate set of constraints on the nodal stresses. In the lower bound finite-element analysis, statically admissible stress discontinuities are permitted at edges shared by adjacent triangles and also along borders between adjacent rectangular extension elements [17].The finite element lower bound limit analysis techniques developed by Lyamin and Sloan [17]and Krabbenhoft et al. [18] provide a useful method for dealing with the problems of slope stability [17]. These numerical lower bound methods have been used to provide chart solutions by Yu et al. [19] for 2D purely cohesive and cohesive-frictional soil slopes. In this paper, similar formulations are used and described with newly types of elements and the effects of seismic forces are also searched through current solution in three dimensional slopes.

By using both lower and upper bound analyses to estimate slope stability, Kim et al. [20] proposed sets of stability charts for inhomogeneous soil slopes and cohesive-frictional soil slopes subjected to pore pressure and seismic loadings respectively. However, their studies were only focused on investigating the stability of 2D slopes. The purpose of the paper is to extend these charts to 3D seismic slope stability problems. Both upper and lower bounds are employed here, and thus true failure load can be bounded.

3. PROPOSED SOLUTION

Consider a body with a volume V and surface area A, as shown in Fig. 2. Let t and q denote, respectively, a set of fixed tractions acting on the surface area A_t and a set of unknown tractions acting on the surface area A_q. Similarly, let g and h be a system of fixed and unknown body forces which act, respectively, on the volume V. Under these conditions, the objective of a lower bound calculation is to find a stress distribution which satisfies equilibrium throughout V, balances the prescribed tractions t on A_t, nowhere violates the yield criterion, and maximizes the integral.

$$Q = \int_{A_q} q \, dA + \int_V h \, dV \tag{1}$$

Since this problem can be solved analytically for a few simple cases only, we seek a discrete numerical formulation which can model the stress field for problems with complex geometries, inhomogeneous material properties, and complicated loading patterns. The most appropriate method for this task is the finite element method.
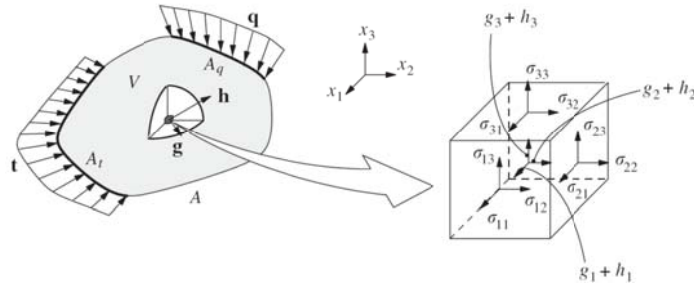
Fig. 2. A body subjected to the surfaces and body forces [17]

Disregarding, for the moment, the type of element that is used to approximate the stress field, any discrete formulation of the lower bound theorem leads to a constrained optimization problem of the form [17];

$$*\text{Maximize } Objective\ Function\ f_j(x) \le 0, \quad j \in J = \{1, \ldots, r\} \tag{2}$$

$$\text{Subject to} \quad a_i(x) = 0, \quad i \in I = \{1, \ldots, m\}$$
$$x \in R^n$$

Where x is an n-dimensional vector of stress and body force variables. The equalities defined by the functions a_i follow from the element equilibrium, discontinuity equilibrium, and boundary and loading conditions, while the inequalities defined by the functions f_j arise because of the yield constraints and the constraints on applied forces. Here, *Objective Function* is described as safety factor of a three dimensional slopes and a_i is a global matrix which contains equilibrium, discontinuity and boundary equations. In addition, f_j produces the conditions which nodal stresses will be less than the yield surface. Maximizing *Objective Function* leads to using an optimization approach. In this paper the nonlinear optimization based on a fast quasi-Newton method whose iteration count is largely independent of the mesh refinement, is selected for finding the maximum lower-bound solution of safety factor which satisfies the element equilibrium, discontinuity equilibrium, and boundary and loading conditions.

4. NEWLY METHOD OF MESH GENERATION

The global form of each element in this solution is shown in Fig. 3.As it is seen the stresses variation between each node of element is assumed to be linear, thus this type of finite element is called *Linear Finite Element*. The following section gives a detailed description of the discretization procedure for the case of 3-dimensional linear elements. There are strong reasons for choosing linear finite elements, and not higher order finite elements, for lower bound computations mentioned by Lyamin and Sloan [17].
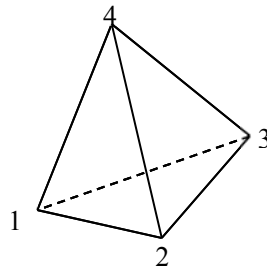

Fig. 3. Global form of elements

Unlike the usual form of the finite element method in which each node is unique to a particular element, multiple nodes can share the same coordinates, and statically admissible stress discontinuities are permitted at all inter-element boundaries. The typical 3D slope geometry details for the problem of this paper are shown in Fig. 4.
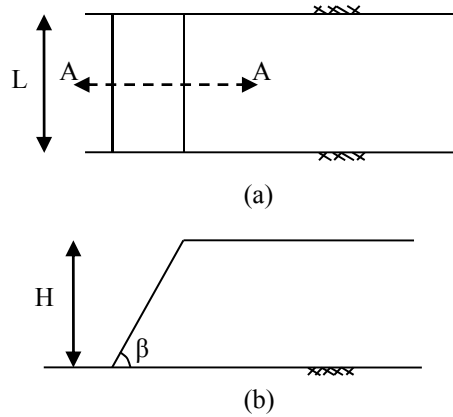
(a)

(b)

Fig. 4. Geometry details of problem (a). Plan (b). Section A-A

In this paper, all models are organized from some prismatic units as is shown in Fig.5. Using this type of unit as a base of modelings, all kind of straight, convex, concave and every other arbitrary shape in plan view of slopes can be created. Each discussed unit is combined from three volumetric pyramid elements which are shown in Fig. 6.
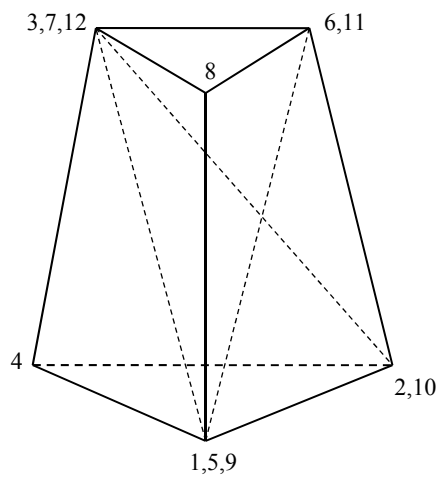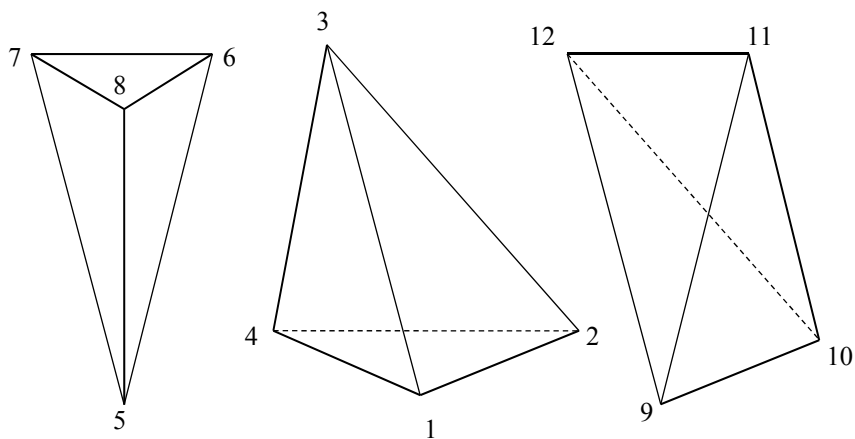

Fig. 5. Prismatic unit of modelings

Fig. 6. Elements used for lower bound limit analysis

The global form of modellings consists of two plans which one locates at the top and the other at the bottom of the model. Figure 7 shows the top and bottom plans of modelling. Between each pair of slices in

the plans (1 to 12), 3 elements in the form of a prismatic unit shown in Fig. 5 are constituted. For higher slopes, various numbers of prismatic units are used in the height of the slopes.

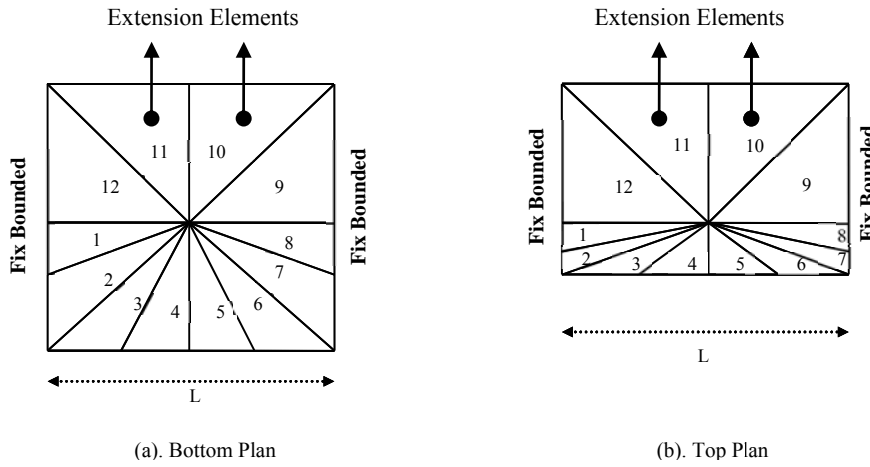(a). Bottom Plan   (b). Top Plan

Fig. 7. Bottom and top plans of modelling, extension of the stress fields into a semi-infinite domain

The typical 3D slope model for the problem of this paper is shown in Fig. 8. This model consists of 12 units and therefore 36 elements.
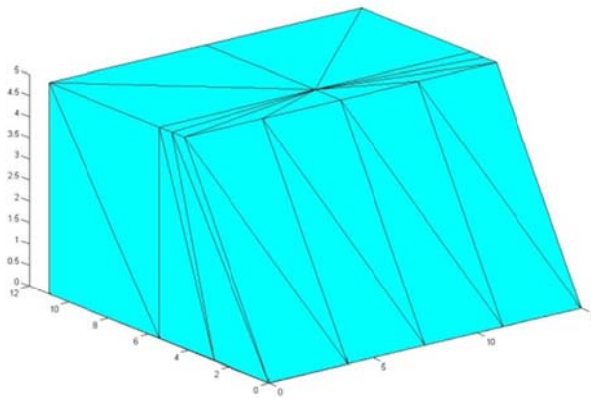

Fig. 8. Finite element model

The extension elements may be used to extend the solution over a semi-infinite domain and therefore provide a complete statically admissible stress field for infinite half-space problems. In fact, the extension elements shown in Fig. 7 can be used readily to extend the stress fields into a semi-infinite domain. Because this paper is concerned mainly with the stability of finite slopes resting on a firm base, extension elements are needed only behind the slopes (shown in Fig. 7).

5. OBJECTIVE FUNCTION AND LOADING CONSTRAINTS

The purpose of lower bound limit analysis is to find a statically admissible stress field which maximizes the *objective function* carried by a combination of surface tractions and body forces (Fig. 2). The distribution of the latter may either be known or unknown, depending on the problem. In the terminology of slopes stability, safety factor is known as the objective function, since this is the quantity, the aim is to maximize in lower bound case. Otherwise the general form of the yield condition for a perfectly plastic solid has the form

$$f(\sigma_{ij}) \leq 0 \tag{3}$$

Where f is a convex function of the stress components and material constants. The solution procedure presented later in this paper does not depend on a particular type of yield function, but does require it to be convex and smooth. Convexity is necessary to ensure the solution obtained from the optimization process is the global optimum, and is actually guaranteed by the assumptions of perfect plasticity. Smoothness is essential because the solution algorithm needs to compute first and second derivatives of the yield function with respect to the unknown stresses. For yield functions which have singularities in their derivatives, such as the Mohr–Coulomb criteria, it is necessary to adopt a smooth approximation of the original yield surface. A plot of this function in the meridional plane is shown in Fig. 9.
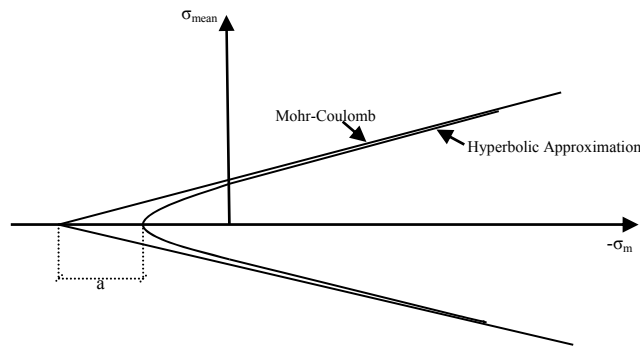

Fig. 9. Hyperbolic approximation to Mohr–Coulomb yield function

Defining tensile stresses as positive, the Mohr-Coulomb yield function may be written as

$$f = (\sigma_1 - \sigma_2) + (\sigma_1 + \sigma_2)sin\emptyset_d - 2c_d cos\emptyset_d \tag{4}$$

where the principal stresses are ordered so that $\sigma_1 > \sigma_2 > \sigma_3$ and c_d and $\emptyset_d$ are

$$Fs_c = c/c_d \tag{5}$$

$$Fs_\emptyset = \tan(\emptyset)/\tan(\emptyset_d) \tag{6}$$

Which C and $\emptyset$ denote, respectively, the cohesion and friction angle of the soil. Assuming $Fs = Fs_c = Fs_\emptyset$ the objective function defined as maximizing the safety factor by satisfying the yield function. This implies that the stresses at all nodes in the finite element model must satisfy the yield condition.

Thus, in total, the yield conditions give rise to some non-linear inequality constraints (considering composite yield criteria as one constraint) on the nodal stresses. Because each node is associated with a unique set of stress variables, it follows that each yield inequality is a function of an uncoupled set of stress variables σ_{ij}^l. Each admissible stress field has its own safety factor. Using an optimization method of nonlinear programming which is based on Newton's method the highest lower bound safety factor is attained. In this method, the non-linear equations at the current point k are linearized and the resulting system of linear equations is solved to obtain a new point k + 1. The process is repeated until the governing system of non-linear equations is satisfied. Thus, the highest lower bound safety factor of admissible stress fields is searched; this feature can be exploited to give a very efficient solution algorithm.

When the lower bound method described previously is applied to problems with semi-infinite domains, only part of the body is discretised. To cover the stress fields conditions in semi-infinite zones some extension elements are deployed around the periphery of the meshes. These are constructed so that they extend the stress field beyond the limits of the grid in such a way that it is statically admissible [17]. The proposed algorithm is concerned with the following domains:

1. Mesh generating using the plans above and below

2. Deriving equilibrium, discontinuity and boundary matrices for each element
3. Deriving A_{global} which attains following equation:

$$A_{\text{global}}x^e = b_{\text{global}} \tag{7}$$

Where x^e is unknown vector which includes the stresses in each node and *the safety factor*.

4. Optimizing process: This optimization is ascribing to check the maximum lower bound solution using nonlinear programming.
5. Constraints: This algorithm contains both equality and inequality constraints. The equality constraint is summarized in a global matrix containing equilibrium, discontinuity and boundary equations and the inequality constraints are refer to a) Yield Surface and b) Extension elements.

The typical lower bound finite element meshes and boundary conditions used to analyze the 3D slope problem are illustrated in Fig.8. The stability of homogeneous slopes is usually expressed in terms of two dimensionless stability numbers in the following form

$$N_s = \gamma H F_s / c \tag{8}$$
$$\lambda_{\phi c} = N_s \tan\phi / F_s \tag{9}$$

Where *Ns* is the stability number, γ is the soil unit weight, *H* is the slope height, *Fs* is the safety factor of the slope. Also, *c* and Φ are known as the strength parameters of the material; c represents the cohesion and Φ represents the angle of internal friction.

6. COMPARISON WITH OTHER RESULTS

One of the most important parameters in analyzing is number of used elements in models. Certainly, increasing this quantity leads to an increase in the accuracy of the results. But using a high number of elements in modelling causes time consuming runs, therefore some models were made to compare the results by different number of elements.

For constant quantity of k_h=0.3, β=30 and $\lambda_{\phi c}$=2, the results for En=18,24,36 and 72 shown in Fig. 10 are compared, where k_h is seismic coefficient, β is degree of the slope and En is number of used elements. As is seen, an increase in element numbers results in decreasing the interspaces between lower bound and upper bound solutions, it means that by increasing the element numbers, the accuracy of the results is increased but its rate decreases, as Fig.10 shows. Therefore, it can be concluded that for higher number of elements, the difference between results can be connivance. Thus in this paper, all numerical results are made of 36 elements because of low rate of variations afterwards.

For validation, the results of the current approach can be compared with those of other investigators for slopes in static cases. Different methods have been proposed for 3D analysis of straight slopes by Baligh and Azzouz [21], Hovland [22], Chen and Chameau [23], Ugai [24], Leshchinsky and Baker [25] and Totonchi et al [26-28]. Comparing the current results with most of these, good agreement is found among them. Ugai [24] extended Baker variational limiting equilibrium approach to 3D cohesive slopes. Leshchinsky and Baker [25] extended a modified solution of variational approach in 3D stability of slopes which has been proven to be equivalent to the upper bound solution in the framework of limit analysis. Totonchi et al. [26, 27] used this method of solution for computing the stability of curved slopes and acceptable stress field in retaining walls during seismic loading.

Figure 11 shows the ratio *F_{3D}/F_{2D}* (*F_{iD}* is the safety factor in *iD* analysis) as a function of *L/H* obtained by Ugai [24], Leshchinsky and Baker [25], Farzaneh and Askari [6] (the upper-bound solution) and the present solution. According to the upper bound results and the results of the current solution, it is

found that these results can bracket the slope stability numbers to ±9% and therefore can be used to benchmark for solutions from other methods.
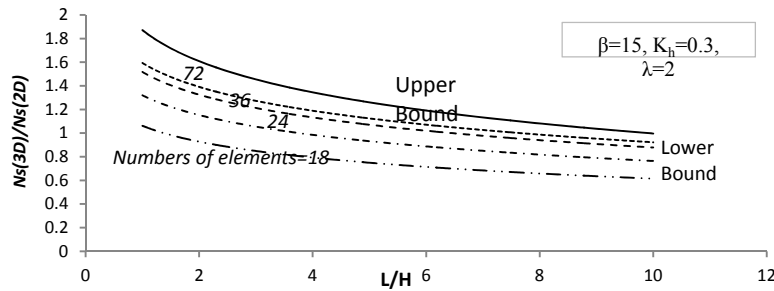
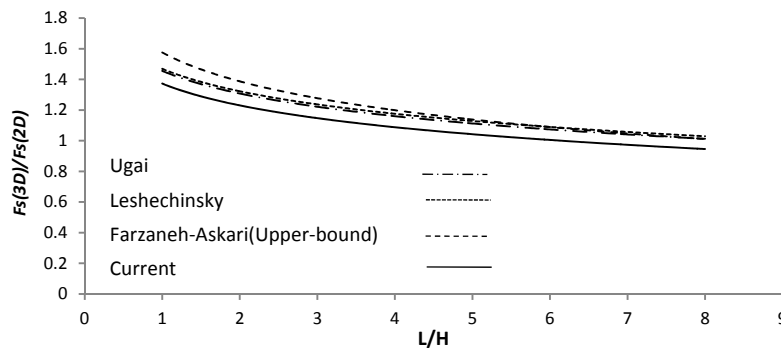

Fig. 10. Effect of element numbers in accuracy of results

Fig. 11. Comparison with those of Ugai, Leshchonsky, Farzaneh-Askari in cohesive soil

7. NUMERICAL RESULTS AND DISCUSSIONS

a) *Stability charts for homogeneous slopes based on the numerical limit analyses*

The 3D chart solutions for homogeneous slopes due to earthquake forces obtained from the numerical upper and lower bound analysis are displayed in Figs. 12-16for a range of slope angles *(β),* seismic coefficients *(kₕ),* and *L/H* ratios. It can be noted that the upper and lower bound limit analysis solutions bracket a range of stability numbers *(Nₛ)* to within ±9% or better for 3D cases. The upper bound results were collected from Farzaneh and Askari [7].

As expected, the stability number N_s decreases when *β* and the *L/H* ratio increase. For a given *β* and k_h, N_s achieves the minimum value when *L/H* goes to infinite. This implies that the factor of safety will reduce with increasing *L/H* ratio. As is known, the plain strain analysis does not consider the resistance provided by the two curved ends of the slip surface. The boundary resistance from these two curved ends can be seen as 3D end boundary effect which makes the slope more stable. While increasing the *L/H* ratio, the relative contributions of resistances provided by these two curved ends decrease, which means that 3D end boundary effect reduces. Therefore, using 2D stability numbers will lead to a more conservative slope design. Fig. 12-16 illustrate the ratio of stability numbers obtained from 3D Lower and upper bound solutions to stability numbers obtained from 2D upper bound analysis (indicated in Table 1).These numbers can be used for estimating the seismic stability of the slopes without retaining walls and props.

A comparison of the equivalent 2D and 3D cases can be made by investigating the factor of safety ratio F3D/F2D for the same slope angle (β), seismic coefficient (*kₕ*), slope height (H), unit weight (γ) and dimensionless parameter (*λ_φc*). The ratio F_{3D}/F_{2D} is simply the ratio of the stability numbers $(N_s)_{2D}/(N_s)_{3D}$. Figure 17 shows a sample average of the upper and lower bound ratio of *F₃D/F₂D* for various seismic coefficients *(kₕ)* and *L/H*. In this figure, the magnitude of *F₃D/F₂D* denotes the degree in which the 2D analysis underestimated the slope stability. It should be acknowledged that the true ratio of *F₃D/F₂D*has

been bracketed by the numerical upper and lower bound analysis within a range of ±9%.Referring to Fig. 17, the ratio of F_{3D}/F_{2D} is found to increase with increasing k_h, and decreasing L/H.

Chugh [29] analyzed a sample problem and pointed out that the difference between 2D and 3D safety factors tends to lose significance when $L/H > 5$. However, in some conditions the results of the current study give the F_{3D}/F_{2D} ratio as high as 1.1 for the uniform slopes when $L/H = 5$. The difference between the 2D and 3D factor of safety estimates is greater than 10% which would be important and is not negligible for the back analysis of a failed slope in practice.

Table 1. 2D stability numbers from upper bound solutions (λ=2)

k_h	β				
	15	30	45	60	90
0	18.7	12.9	10.3	8.4	5.52
0.1	13.1	10.5	8.84	7.44	5.02
0.2	9.9	8.72	7.66	6.6	4.54
0.3	7.62	7.36	6.7	5.88	4.19

b) Example of application

In order to make comparisons of the factor of safety between the newly proposed 3D chart solutions and the 2D, an example is introduced. The slope descriptions are as follows: the slope inclination β=60, the height of the slope is H = 4 m, width of the slope is L=16 m, the seismic coefficient is k_h=0.2, the soil unit weight is γ = 17kN/m3, the friction angle is Φ =17 degree and the cohesion is 10 kPa.
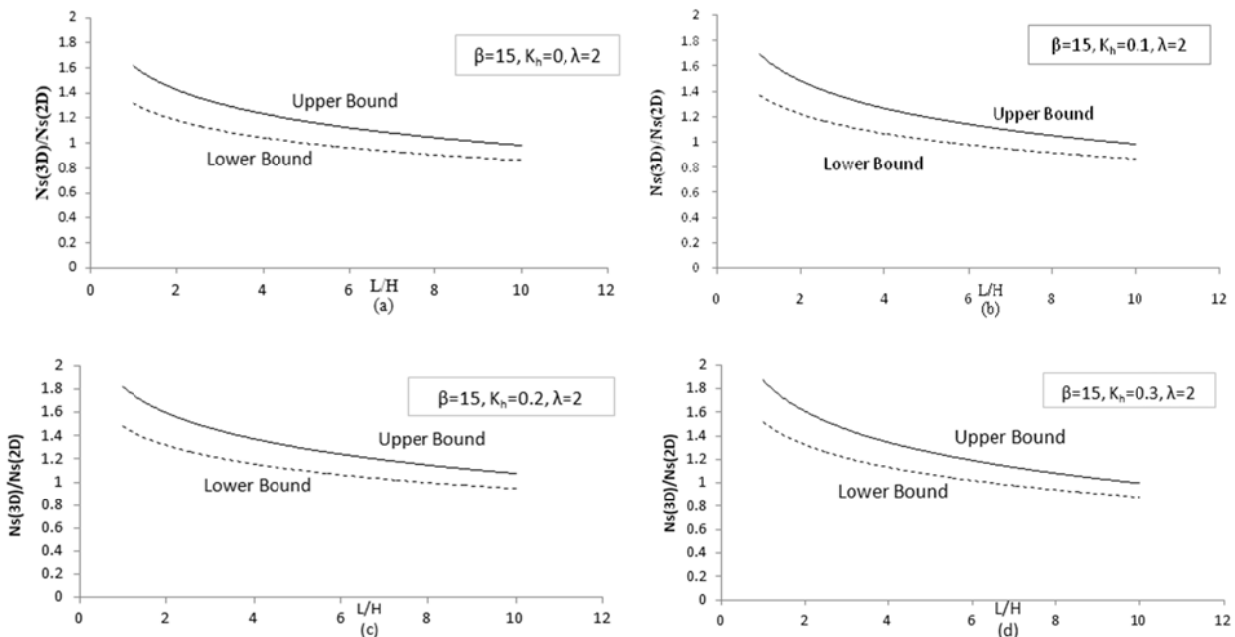

Fig. 12. Limit analysis solution of seismic stability numbers for β=15, λ=2
and (a).kh=0, (b). kh=0.1, (c). kh=0.2,(d). kh=0.3

A procedure for obtaining the factor of safety by using the chart solutions presented in this study can be summarized in the following stages.

1. From the slope descriptions, the non-dimensional parameters are λ= (17×4/10)×tan 17=2. One of the constraints for using the explained charts is that they are just for λ=2 but no other cases. This constraint can be removed by running more models and preparing some comprehensive charts.

2. For $\beta = 60°$ and $k_h = 0.2$, the chart solutions shown in Fig. 15c is employed to determine the safety factor.

3. In Fig. 15c, a straight line passing through the L/H=4 is plotted. This straight line intersects with the upper and lower bound curves, which are the 3D chart solutions of the numerical limit analysis.

4. The stability number from 2D limit equilibrium method is $N_{s(2D)} = 6.6$. From these intersection points, it can back-figure the dimensionless parameter $N_s(3D)/N_s(2D)$ from which the lower bound solution becomes $Fs_{(Lower\ bound)} = 0.92$ and the upper bound solution becomes $Fs_{(upper\ bound)} = 1.11$.
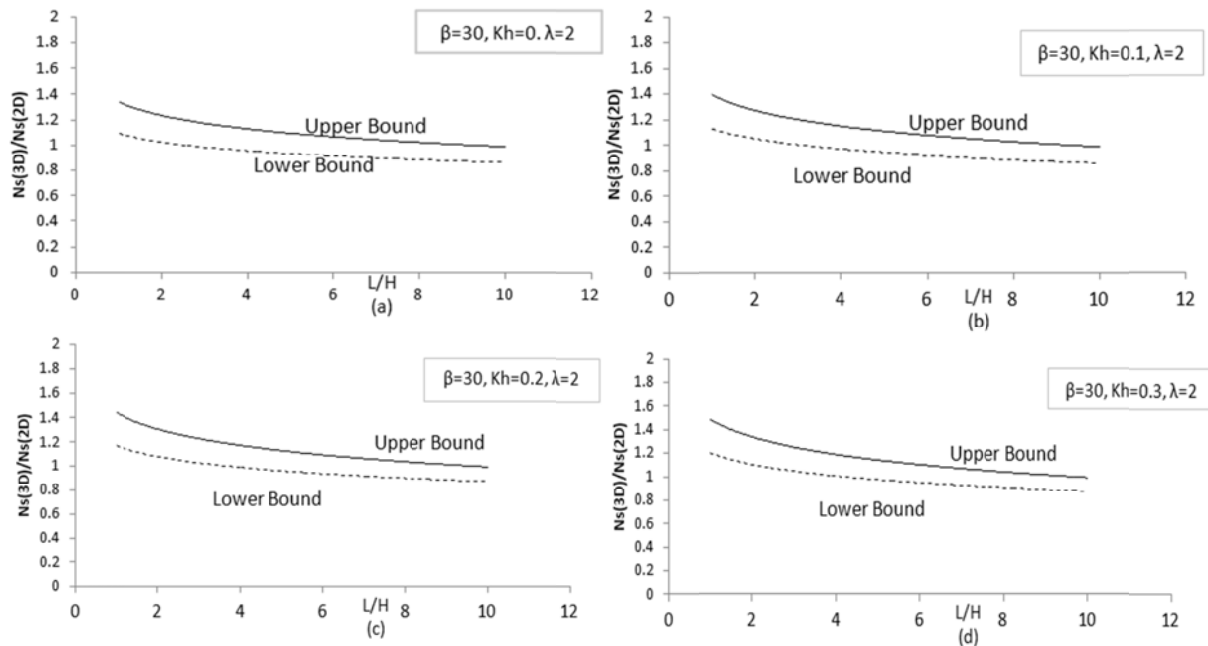

Fig. 13. Limit analysis solution of seismic stability numbers for β=30,
λ=2 and (a).kh=0, (b). kh=0.1, (c). kh=0.2,(d). kh=0.3
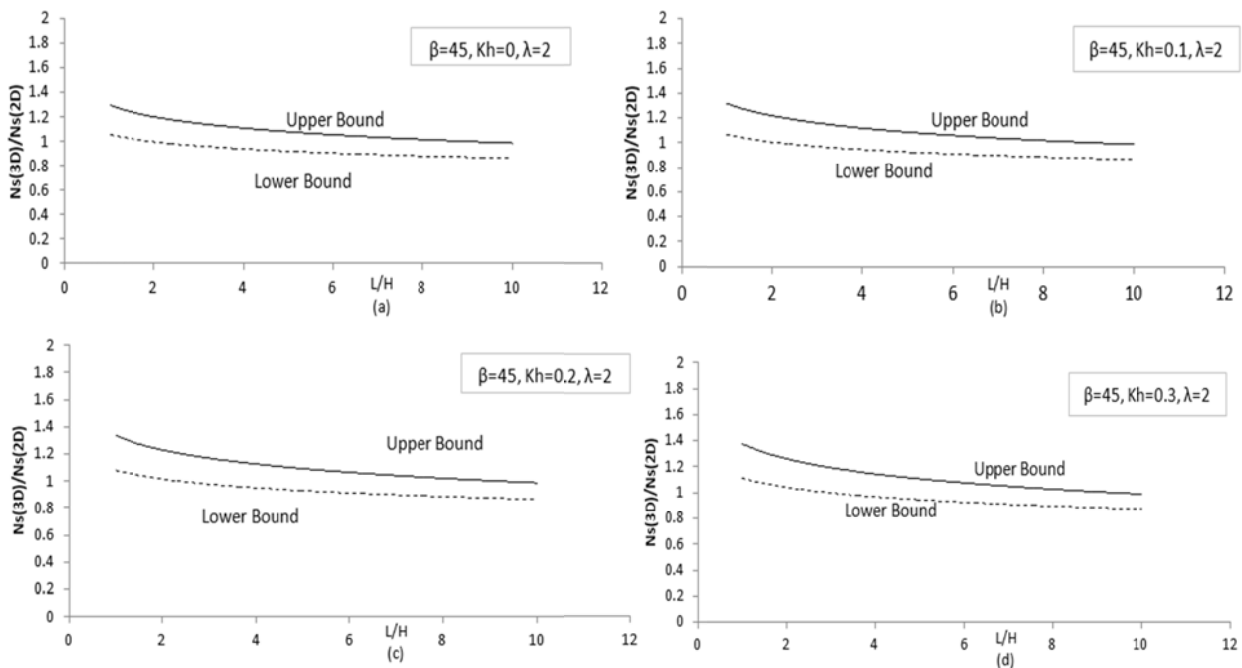

Fig. 14. Limit analysis solution of seismic stability numbers for β=45,
λ=2 and (a).kh=0, (b). kh=0.1, (c). kh=0.2,(d). kh=0.3

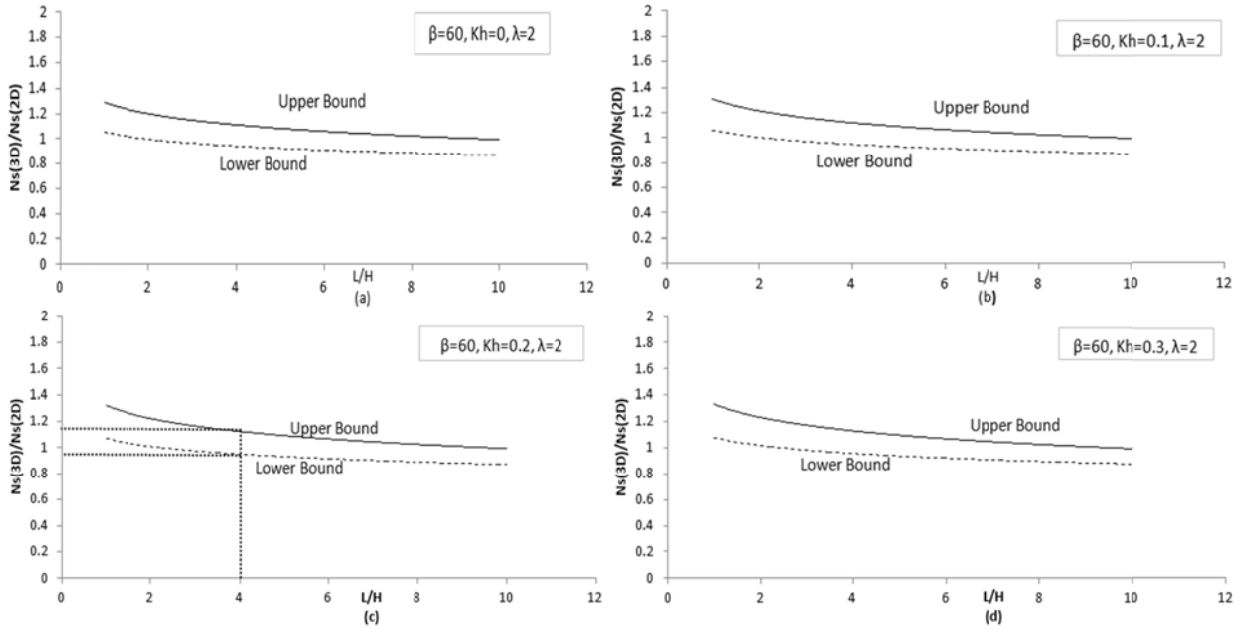Fig. 15. Limit analysis solution of seismic stability numbers for β=60,
λ=2 and (a).kh=0, (b). kh=0.1, (c). kh=0.2,(d). kh=0.3

The average of the upper and lower bound safety factors is 1.015 for *L/H* =4, considering others conditions for L/H = 1, *L/H* = 2 and *L/H* = 3; the average of safety factors come to 1.16, 1.11 and 1.067 respectively. The safety factors for the 3D solutions are around 1 to 1.16 times that of the safety factors of the 2D solutions. This demonstrates that the factor of safety obtained from 3D analysis will always be larger or equal to that obtained from 2D analysis. Therefore, using 2D solution is conservative for design and non-conservative when determining strength parameters from a back analysis of a failed slope. In addition, the difference between the upper and lower-bound factors of safety for this example is found to be around 16%. This difference decreases slightly when the ratio of *L/H* increases.
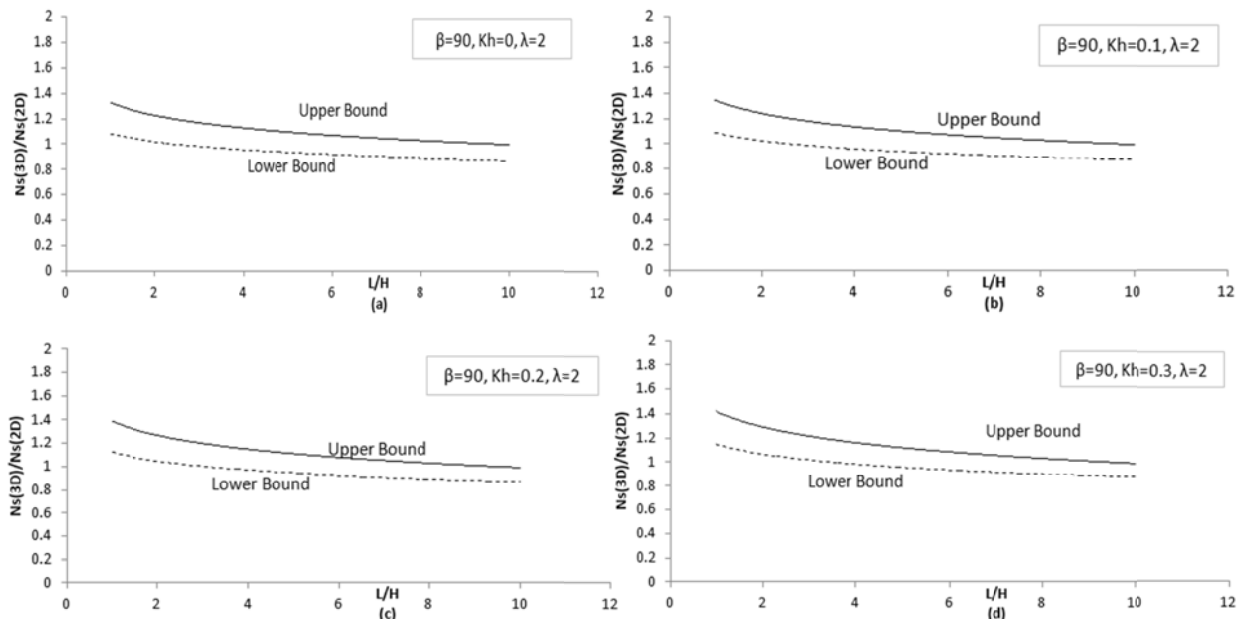

Fig. 16. Limit analysis solution of seismic stability numbers for β=90,
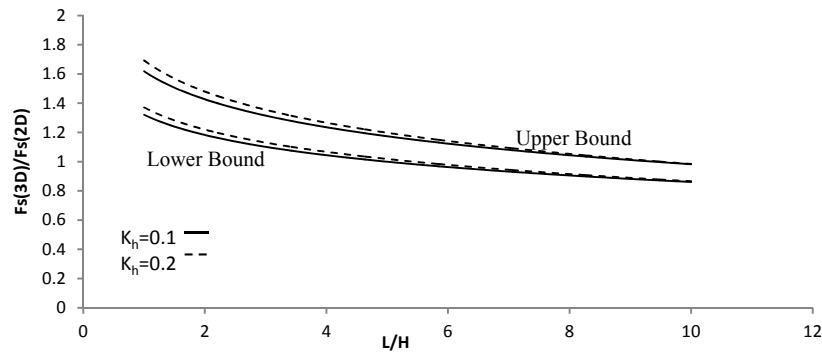λ=2 and (a).kh=0, (b). kh=0.1, (c). kh=0.2,(d). kh=0.3

Fig. 17. Limit analysis solution of seismic stability numbers for β=15, λ=2

8. CONCLUSION

Several studies have indicated that the factor of safety from a 3D analysis will be greater than that from a 2D analysis. This has been proved based on the comparisons between 2D and 3D limit analysis solutions for the factors of safety in both seismic and static cases.

Three dimensional stability charts for homogeneous cohesive slopes have been proposed in this paper. Based on the results presented, the following conclusions can be made:

1. It should be noted that the true ratio of F_{3D}/F_{2D} has been bracketed by the numerical upper and lower bound analysis within a range of ±9% or better for all cases considered. The ratio of F_{3D}/F_{2D} is found to increase with increasing k_h, decreasing β and decreasing *L/H*.

2. For the application example presented, the difference between the upper and lower bound factors of safety is found to be around 16% and for other quantities of L/H, the safety factors for the 3D solutions are around 1 to 1.16 times that of the safety factors of the 2D solutions.

3. The stability number N_s decreases when β and the *L/H* ratio increase. For a given β and k_h, N_s achieves the minimum value when *L/H* goes to infinite. This implies that the factor of safety will reduce with increasing *L/H* ratio.

4. The interspace between upper and lower bound of solutions tends to decrease by increasing *L/H*. It means that for 2D slopes these solutions have the least difference. Inversely for low quantities of *L/H(L/H=1),* this difference goes to be maximum.

REFERENCES

1. Bishop, A. W. (1955). The use of slip circle in stability analysis of slopes. *Geotechnique*, Vol. 5, No. 1, pp. 7–17.

2. Janbu, N. & Bjerrum, L. et al. (1956). Soil mechanics applied to some engineeringproblems. *Norwegian Geotechnical Institute. Publication*, Vol. 16.

3. Gens, A. & Hutchinson, J. N. et al. (1988). Three-dimensional analysis of slides incohesive soils. *Geotechnique*, Vol. 38, No. 1, pp. 1–23.

4. Spencer, E. (1976). A method of analysis of the stability of embankments assuminginter-slice forces. *Geotechnique*, Vol. 17, No. 1, pp. 11–26.

5. Morgenstern, N. (1963). Stability charts for earth slopes during rapid drawdown. *Geotechnique*, Vol. 13, pp. 121–31.

6. Farzaneh, O. & Askari, F. (2003). Three-dimensional analysis of nonhomogeneous slopes. *J. Geotech. Geoenviron. Eng. ASCE*, Vol. 129, No. 2, pp. 137–45.

7. Farzaneh, O. & Askari, F. (1994). 3D stability of slopes using upper bound limit analysis method. PhD Thesis, Tehran University.

8.   Duncan, J. M. (1996). State of the art: limit equilibrium and finite-element analysis of slopes. *J. Geotech. Eng. ASCE*, Vol. 129, No. 2, pp. 577–96.

9.   Chen, J. & Yin, J. H. et al. (2003). Upper bound limit analysis of slope stability using rigidfinite elements and nonlinear programming. *Can Geotech J.*, Vol. 40, pp. 742–52.

10. Chen, Z. & Wang, X. et al. (2001). A three-dimensional slopestability analysis method using the upper bound theorem part I: theory andmethods. *Int J Rock Mech Mi.n Sci.*, Vol. 38, pp. 369–78.

11. Donald, I. B. & Chen, Z. Y. (1997). Slope stability analysis by the upper bound approach:fundamentals and methods. *Can Geotech J*, Vol. 34, pp. 853–62.

12. De Buhan, P. & Garnier, D. (1998). Three dimensional bearing capacity analysis of afoundation near a slope. *Soils Found,* Vol. 38, No. 3, pp. 153–63.

13. Michalowski, R. L. (1989). Three-dimensional analysis of locally loaded slopes. Geotechnique, Vol. 39, No. 1, pp. 27–38.

14. Michalowski, R. L. (2002). Stability charts for uniform slopes. *J. of Geotech. Geoenviron. Eng. ASCE*, vol. 128, No. 4, pp. 351–5.

15. Viratjandr, C. & Michalowski, R. L. (2006). Limit analysis of submerged slopes subjected towater drawdown. *Can Geotech J.*, Vol. 43, pp. 802–14.

16. Michalowski, R. L. (1997). Stability of uniform reinforced slopes. *J Geotech. Geoenviron. Eng. ASCE*, Vol. 123, No. 6, pp. 546–56.

17. Lyamin, A. V. & Sloan, S. W. (2002). Lower bound limit analysis using non-linear programming. *Int J Numer Methods Eng*, Vol. 55, pp. 573–611.

18. Krabbenhoft, K. and Lyamin, AV. et al. (2005). A new discontinuous upper bound limit analysis formulation. *Int J Numer Methods Eng.*, Vol. 63, pp. 1069–88.

19. Yu, H. S. & Salgado, R.et al. (1998). Limit analysis versus limit equilibrium for slope stability. *J Geotech Geoenviron Eng ASCE*, Vol. 124, No. 1, pp. 1–11.

20. Kim, J. & Salgado, R. et al. (1999). Limit analysis of soil slopes subjected to pore-waterpressures. *J Geotech Geoenviron Eng ASCE*, Vol. 125, No. 1, pp. 49–58.

21. Baligh, M. & Azzouz, A. S. (1975). End effects on stability of cohesive slopes. *J. Geotech. Engrg. Div.*, Vol. 101, No. 11, pp. 1105–1117.

22. Hovland, H. J. (1977). Three-dimensional slope stability analysis method. *J GeotechEngDiv ASCE*, Vol. 103, No. 9, pp. 971–86.

23. Chen, R. H. & Chameau, J. L. (1982). Three-dimensional limit equilibrium analysis of slopes. *Geotechnique*, Vol. 32, No. 1, pp. 31–40.

24. Ugai, K. (1985). Three-dimensional stability analysis of vertical cohesive slopes. *Soils Found*, Vol. 25, No. 3, pp. 41–8.

25. Leshchinsky, D. & Baker, R. (1986). Three-dimensional slope stability: end effects. *Soils Found*, Vol. 26, No. 4, pp. 98–110.

26. Totonchi, A., Askari, F. & Farzaneh, O. (2012). 3D stability analysis of concave slopes in plan view using linear finite element and lower bound method. *Iranian Journal of Science and Technology, Transactions of Civil Engineering*, Vol. 36, No. C2, pp. 181-194.

27. Totonchi, A., Askari, F. & Farzaneh, O. (2012). Analytical solution of seismic active lateral force in retaining walls using stress fields. *Iranian Journal of Science and Technology, Transactions of Civil Engineering*, Vol. 36, No. C2, pp. 195-207.

28. Totonchi, A., Askari, F. & Farzaneh, O. (2012). 3D stability analysis of convex slopes in plan view using linear finite element and lower bound method. *International Journal of Civil Engineering*, Vol. 10, No. 2.

29. Chugh, A. K. (2003). On the boundary conditions in slope stability analysis. *Int J Numer Anal Methods Geomech*, Vol. 27, pp. 905–26.